Simulations of gap-soliton generation

C. Martijn de Sterke
School of Physics, University of Sydney, Sydney, New South Wales 2006, Australia
and Optical Fibre Technology Centre, University of Sydney, Sydney, New South Wales 2006, Australia
(Received 12 June 1991)

Numerical results are presented showing the generation of gap solitons by external pulses incident on a nonlinear periodic medium. It is shown that the required energy strongly depends on whether the effective index of the periodic structure is well matched to the refractive indices of the surrounding media.
PACS number(s): 42.50.Rh, 42.65.−k

I. INTRODUCTION

Gap solitons were discovered in 1987 while studying the properties of periodic media with a Kerr-like nonlinearity [1]. Since this discovery the time-independent properties of gap solitons have received the most attention. This work has led to the understanding that stationary gap solitons can be created by sufficiently powerful cw radiation incident on a nonlinear periodic medium. Subsequent fully time-dependent analyses have shown that this picture is incomplete: An instability can occur, preventing the system from ever settling in a stationary state [2, 3]. Rather, if the incoming cw radiation is sufficently intense, the systems exhibit self-pulsing, which can turn chaotic at yet higher intensities.

In the present paper the dynamical properties of nonlinear periodic media are studied differently: The incoming radiation is pulsed, and the pulse length is of the order of the round-trip time of the system preventing it from settling even if the instability were absent. Pulsed inputs have been considered before [4], but there the amplitude and the phase of the pulse were carefully chosen so as to generate a gap soliton with prescribed parameters. In contrast, here the input pulse is not preselected in this way—in fact, it is just a Gaussian with uniform phase. It is especially this phase function which makes the numerical simulations here quite different from the results presented before [4] (this distinction is similar to that observed in the switching characteristics of solitons and of simple square pulses in nonlinear Sagnac interferometers [5]). If the peak power of the incident pulses is low, then the periodic nonlinear stack behaves as if it was linear and, since most of the energy falls inside the rejection band of the periodic structure, most of the energy is reflected. For higher incoming powers a gap soliton can form near the front of the system. It subsequently moves to the back (cf. Ref. [2]), releasing most of its energy in a single burst. As previously discussed by Winful [6], this leads to significant pulse reshaping and, under suitable conditions, to pulse compression.

In these investigations it is important that a significant fraction of the incoming indeed does enter the system and contributes to the formation of the gap soliton. Similarly, to facilitate detection it is important that once a gap soliton has formed and has traveled to the back of the system, a substantial fraction of the energy leaves the periodic medium so that it can be detected. In this paper special emphasis is given to these matters. Though it is at present unknown what determines the parameters of the gap soliton which is formed when an arbitrary pulse is incident onto a nonlinear periodic medium, the present work shows that the choice of refractive indices and thicknesses of the outer layers are crucial in optimizing the energy transfer between gap solitons and the surrounding media.

The outline of this paper is as follows. In Sec. II some key properties of linear periodic media are reviewed. In Sec. III results of numerical simulations are presented. The results from Sec. II are used here to understand the energy transfer through the stack. Finally, the results are discussed in Sec. IV.

II. PROPERTIES OF LINEAR PERIODIC MEDIA

In this section I review some of the key properties of linear periodic structures. Such a geometry is shown schematically in Fig. 1. It is true that such structures

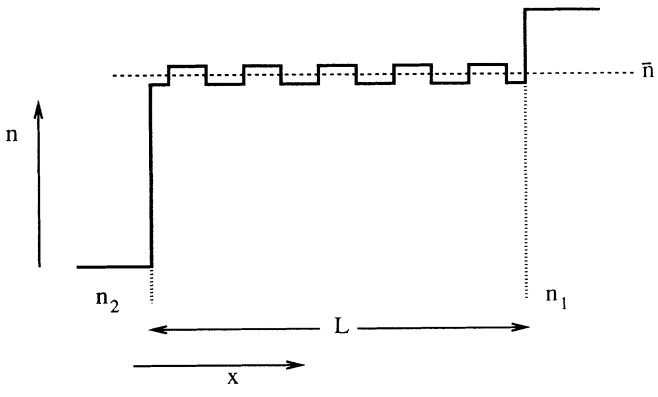

FIG. 1. Schematic of the periodic stack considered here. The incoming energy comes from the left in this figure and is thus incident through medium 2. As mentioned in the text, using coupled-mode theory only the lowest Fourier component of the index distribution is included. Note that $\bar{n}$ is defined in Eq. (3).

have been widely studied, particularly in the context of thin-film optics, where they are used in highly reflective coating and in edge filters [7], as well as in that of integrated optics, for determining the properties of corrugated waveguides. For corrugated waveguides one often has $n_1 = n_2 = \bar{n}$ (see Fig. 1). In addition, the modulation depth is often small enough for coupled-mode theory to be used, leading to analytic results for, say, the reflectivity. But in thin-film optics such simplifications are often not allowed—indeed the modulation depth can be of order unity [7], so that numerical techniques must be used, and the n_i often differ from $\bar{n}$.

Here I discuss a situation in which the modulation depth of the stack is small enough for coupled-mode theory to be used, but $n_1 \neq n_2 \neq \bar{n}$. In addition, while the stack is taken to have an integer number of periods, the material and thickness of the first layer, and therefore that of the last layer too, are not fixed. This is expressed by the parameter φ in the distribution of the dielectric constant:

$$\epsilon(x) = \bar{\epsilon} + \Delta\epsilon\, \mathrm{U}(x/d + \varphi/2\pi) \ , \tag{1}$$

where the factor 2π was introduced for future convenience, and, with N an integer, where the periodic step function U is defined through

$$U(z) = \begin{cases} +1 & \text{if } -\frac{1}{4} + N < z < +\frac{1}{4} + N \\ -1 & \text{otherwise.} \end{cases} \tag{2}$$

For convenience I also define

$$\bar{n} = \sqrt{\bar{\epsilon}} \tag{3}$$

(see Fig. 1). If $\varphi = \frac{1}{2}\pi$, the stack begins with a full layer of the high-index material and, since the number of periods is integer, ends with a full layer of the low-index material. If $\varphi = \frac{3}{2}\pi$ this is reversed. For $\varphi = 0$, π, the stack is symmetric with outer layers having either the high index ($\varphi = 0$) or the low index ($\varphi = \pi$). The choice of the first and last layers is known to be of considerable importance when $\bar{n} \neq n_1, n_2$ [7], but plays no role when the index difference between the surrounding media and the stack is small.

As mentioned, coupled-mode theory is used to analyze the properties of media with refractive index as in Eq. (1). Since this is a first-order theory, only the lowest Fourier component of the index distribution is included, and coupled-mode theory is thus, strictly speaking, valid only when the modulation depth is small. Nevertheless, it is applied in Sec. III to a stack with $\Delta n \equiv \Delta\epsilon/2\bar{n} \approx 0.30$. Though the validity of coupled-mode theory for such a large modulation depth is questionable, it has the advantage of yielding analytic results which are qualitatively correct. Use of coupled-mode theory has the additional advantage that it is equally applicable to thin-film stacks, waveguides, and optical fibers.

To use coupled-mode theory the electric field is written as

$$E(x,t) = [\mathcal{E}_+(x,t)e^{-i(\omega_0 t - k_0 x)} + \mathcal{E}_-(x,t)e^{-i(\omega_0 t + k_0 x)}]f(y,z) + \text{c.c.} \ , \tag{4}$$

where $k_0 = \pi/d$, ω_0 is the associated angular frequency, and c.c. denotes complex conjugation. The functions $\mathcal{E}_\pm$ are assumed to be slowly varying and are thus envelope functions. The function $f(y,z)$ only depends on the transverse coordinates and represents the particular mode considered. In the case of a thin-film stack this is a uniform function. The modes for optical waveguides and fibers are well known too [8]. Using standard techniques one can find a set of coupled equations for the envelope functions,

$$\begin{aligned} +i\frac{\partial\mathcal{E}_+}{\partial x} + i\frac{\bar{n}}{c}\frac{\partial\mathcal{E}_+}{\partial t} + \kappa e^{-i\varphi}\mathcal{E}_- + \delta\mathcal{E}_+ = 0 \ , \\ -i\frac{\partial\mathcal{E}_-}{\partial x} + i\frac{\bar{n}}{c}\frac{\partial\mathcal{E}_-}{\partial t} + \kappa e^{+i\varphi}\mathcal{E}_+ + \delta\mathcal{E}_- = 0 \ , \end{aligned} \tag{5}$$

where the detuning $\delta = k - k_0$, where k is the actual wave vector of the light. The coupling coefficient κ strongly depends on the geometry. For a thin-film stack, for example, it is given by

$$\kappa = \frac{4}{\pi}\frac{k_0\Delta\epsilon}{4\bar{\epsilon}} \ , \tag{6}$$

where the factor $4/\pi$ is added to obtain the amplitude of the lowest Fourier component of the distribution of dielectric constant in Eq. (1). The coupling coefficients for waveguides and fibers have been given, among others, by Marcuse [8].

It is well known that periodic structures exhibit Bragg reflection, which is associated with a band gap, or rejection band, centered around the frequency ω_0. Using Eqs. (5) it can be shown that the width of this band is $2\kappa c/\bar{n}$. The emphasis in this section is on frequencies just *outside* the gap. These are characterized by $|\delta| > \kappa$—the remaining frequencies ($|\delta| < \kappa$) fall within the gap and are strongly reflected. These frequencies are briefly discussed at the end of the section.

Taking the radiation to be incident through medium 2 (Fig. 1), one can use standard coupled-mode theory to find the amplitude reflection r_S outside the rejection band,

$$r_S = -\frac{r_2 s_- + r_1 r_2 e^{i\varphi} s_0 + r_1 s_+ + s_0 e^{-i\varphi}}{s_- + r_1 e^{i\varphi} s_0 + r_1 r_2 s_+ + r_2 s_0 e^{-i\varphi}} \ , \tag{7}$$

where the r_i are the appropriate Fresnel coefficients

$$r_i = \frac{\bar{n} - n_i}{\bar{n} + n_i} \tag{8}$$

and

$$\begin{aligned} s_0 &= \sin[\sinh(\psi)\kappa L] \ , \\ s_\pm &= \sin[\sinh(\psi)\kappa L \pm i\psi] \ . \end{aligned} \tag{9}$$

Finally, the parameter ψ determines the detuning; it is defined through

$$\cosh(\psi) = \delta/\kappa \ . \tag{10}$$

In the form given here these equations are only valid

for frequencies such that $\delta > \kappa$. But the reflectivity for $\delta < -\kappa$ can be found from those at $|\delta|$ by replacing ψ by $\psi + i\pi$. Then $s_0 \to -s_0$ and $s_\pm \to s_\mp$. To obtain results for frequencies inside the the gap ($|\delta| < \kappa$), ψ should be replaced by $-i\psi$. I return to this below.

Equation (7) shows that if $n_1 = n_2 = \bar{n}$, so that $r_1 = r_2 = 0$, the reflectivity $|r_S|^2$ does not depend on φ. Further interpretation of Eq. (7) is facilitated by an effective-medium approach in which the periodic stack is replaced by a *uniform* medium characterized by a frequency-dependent effective index n_E, optical phase length Δ, and phase shifts φ_i upon reflection off the interfaces with the surrounding media, leaving a geometry similar to a plane-parallel cavity. Indeed, r_S can then be found from an equation which is very similar to the standard expression for the reflectivity of such a system [9]. The effective index n_E of the stack is given by

$$n_E = \frac{1}{ik}\frac{1}{E}\frac{\partial E}{\partial x} = \bar{n}\frac{1 + e^{-i\varphi}e^{-\psi}}{1 - e^{-i\varphi}e^{-\psi}} , \tag{11}$$

where E is a plane wave satisfying Eq. (5). For large detunings $\psi \gg 1$ [see Eq. (10)], and $n_E = \bar{n}$, as required. The equivalent phase length is

$$\Delta = \kappa L \sinh(\psi) . \tag{12}$$

For large detunings, again, $\kappa \sinh(\psi) \approx \delta$ and the well-known expression for the phase shift upon traversing a uniform medium is obtained. Finally, the phase shifts incurred upon reflection off the interfaces with the surrounding media are given by

$$e^{i\varphi_i} = \frac{1 + r_i e^{+i\varphi}e^{-\psi}}{1 + r_i e^{-i\varphi}e^{-\psi}} , \tag{13}$$

which, as expected, vanish for large detunings.

With these definitions the reflectivity r_S in Eq. (7) can be recovered from an expression which differs from that for the reflectivity of a plane-parallel plate [9] only by extra phase shifts φ_i and by the presence of a complex conjugation (indicated by the star) in the denominator:

$$r_S = -\frac{r_2' - r_1' e^{i(2\Delta - \varphi_1 + \varphi_2)}}{1 - r_1'(r_2')^* e^{i(2\Delta - \varphi_1 + \varphi_2)}} , \tag{14}$$

where the r_i' are just the Fresnel coefficients

$$r_i' = \frac{n_E - n_i}{n_E + n_i} . \tag{15}$$

Because of the similarity of Eq. (14) to that for a standard plane-parallel cavity, the reflectivity of the linear stack is now more easily interpreted. The effective optical phase Δ [Eq. (12)] of the stack, which is strongly frequency dependent, results in fringes, which occur when Δ goes through a cycle of 2π. These fringes narrow with increasing stack length L. The stack's reflectivity also depends on n_E. If the $n_1 = n_2 = n_E$, then both r_i' vanish, and the stack has the same index as the surrounding media, resulting in a vanishing reflection, independent of L. Clearly this can only occur if $n_1 = n_2$. This special case is now discussed first.

As mentioned above, if $n_1 = n_2 = n_E$, then the reflectivity of the stack vanishes. This condition can only be satisfied if n_E is real, which requires that $\varphi = 0$ or π, and that [see Eqs. (10) and (11)]

$$\frac{\delta_0}{\kappa} = \mp\frac{\bar{n}^2 + n_i^2}{\bar{n}^2 - n_i^2} , \tag{16}$$

where the top (bottom) sign applies when $\varphi = 0$ (π). Note, again, that Eq. (16) does not depend on L since the effective index of the stack exactly matches the refractive indices of the surrounding media, leading to a suppression of interface reflections [Eq. (15)]. Equation (16) shows that for a given stack (φ fixed) surrounded by media of given refractive index the reflectivity vanishes either for positive or negative values of δ—the grating response is thus asymmetric. Such behavior is well known in thin-film optics, where it is used in the design of edge filters [7]. Note also that in the limit in which $n_i = \bar{n}$ the reflectivity minimum shifts to very large detunings leading to the well-known symmetric response for a waveguide grating. But for large index contrasts $|\delta_0| \to \kappa$, and the reflectivity vanishes at frequencies just outside the rejection zone.

To understand the behavior of the reflectivity at frequencies just around δ_0 it is not very useful to consider Eq. (14), as it contains the rapidly varying fringes. Of more interest is the envelope of the reflectivity, without these fringes. To find the envelope notice from Eq. (14) that if $r_1' = r_2' = r'$ and the exponent equals *unity*, the reflectivity vanishes. This implies that the envelope of the reflectivity r_E can be found by setting the exponential factor equal to -1 in Eq. (14). This substitution and the fact that r' is real then lead to

$$r_E = \frac{2r'}{1 + (r')^2} . \tag{17}$$

Substituting Eqs. (10), (11), (15), and (16) into this expression shows that to lowest order the envelope of the reflectivity R_e is parabolic:

$$R_e = \frac{1}{\left[\left(\frac{\delta_0}{\kappa}\right)^2 - 1\right]^2}\left(\frac{\delta - \delta_0}{\kappa}\right)^2 , \tag{18}$$

with the parabola narrowing as $\delta_0/\kappa \to 1$ (recall that the edge of the gap is at $\delta = \kappa$). Thus if the embedding media at the front and at the back of the system are identical, and if the stack is symmetric, the envelope of the reflectivity vanishes at a frequency outside the central rejection band. For large contrast ratios this frequency is very close to the edge of the gap [Eq. (16)], and the minimum is very narrow [Eq. (18)], while for small contrast ratios the reflectivity vanishes far from the rejection band, and this minimum is now very wide. As discussed in Sec. III an intermediate situation is optimal for the generation of gap solitons.

Now consider the situation in which the media at the front and the back of the system have different indices of refraction ($n_1 \neq n_2$). It is now impossible to match the effective index to that of both of the embedding media at the same frequency. However, matching may be achieved by adding a buffer layer with an optical thickness of $\lambda/4$

and refractive index $\sqrt{n_E n_i}$ [7]. This is used in Sec. III. Notice that if the stack is *not* symmetric ($\varphi \neq 0$ or π) the effective index of the stack is complex [Eq. (11)]. Proper matching is then impossible with dielectric materials.

As mentioned the properties of the stack for frequencies inside the gap can be found from the results presented above by replacing ψ by $-i\psi$. This renders the effective index and the optical phase length to be complex (in the gap the field has exponentially growing and decaying solutions). While matching to dielectric materials is impossible, the reflectivity inside the gap is found to depend on the choice of the n_i and φ: On the side of the gap closest to δ_0 the reflectivity decreases; on the other side it increases.

III. NUMERICAL RESULTS

Although the theory presented in the preceding section strictly speaking only applies to linear systems, it has been found to be useful in the analysis of nonlinear stacks too. It shows a way to optimize the energy transfer between the stack and the surrounding media, allowing a minimization of the external energy required to launch gap solitons and, once a gap soliton is generated, to detect a substantial fraction of the energy it carries.

To understand why the linear properties of the stack are important it is good to recall that gap solitons can exist because the nonlinearity shifts the gap of the linear periodic structure, so that certain frequencies are rejected at low intensities, but transmitted at high intensities [10, 11]. The required intensity is minimized when the frequency content of the incoming pulse, and therefore that of the gap soliton, is close to the high-frequency (low-frequency) edge if the nonlinearity is positive (negative) since then the required shift of the gap is smallest [11]. Since gap solitons consist of frequencies which are inside the gap at low intensities, but outside at high intensities, the stack's response to frequencies close to the edge of the gap is of particular importance. It was shown in Sec. II that for these frequencies the indices of the stack and the surrounding media can be matched. In the linear limit, therefore, these frequencies more easily penetrate the stack, so that less external energy is required for gap-soliton formation. A similar argument holds when considering the opposite process: how to optimize the energy transfer from an existing soliton inside the structure to the surrounding medium when it reaches the back of the structure. Again, the indices of the structure for frequencies just around the gap should match for this process to occur efficiently.

The influence of the index matching described above is illustrated with two sets of numerical results. The first set shows the power-dependent transmissivity to cw radiation of a nonlinear stack. The second set of numerical results show the transmission characteristics for incoming pulses. The parameters for the stack used here are identical to those of Cada *et al.* [13], who in recent experiments studied the behavior of a periodic nonlinear medium, but in a different context. Their stack has 30 periods, each period consisting of a layer of GaAs and AlAs. They use 885-nm radiation, which is just below the band gap of GaAs. Though these choices may not be optimal for studying gap solitons they are used here for illustrative purposes. Though the refractive indices of GaAs and AlAs differ significantly, coupled-mode theory is used for analysis since the results presented are illustrations and since the use of a more general theory is not expected to change the results quantitatively.

In the simulations to study nonlinear periodic media the linear equations Eq. (5) have to be augmented. It is well known [6] that in the presence of a Kerr nonlinearity the coupled-mode equations read [cf. Eq. (5)]

$$+i\frac{\partial \mathcal{E}_+}{\partial x} + i\frac{\bar{n}}{c}\frac{\partial \mathcal{E}_+}{\partial t} + \kappa e^{-i\varphi}\mathcal{E}_- + \delta\mathcal{E}_+ + \Gamma|\mathcal{E}_+|^2\mathcal{E}_+ + 2\Gamma|\mathcal{E}_-|^2\mathcal{E}_+ = 0 ,$$

$$-i\frac{\partial \mathcal{E}_-}{\partial x} + i\frac{\bar{n}}{c}\frac{\partial \mathcal{E}_-}{\partial t} + \kappa e^{+i\varphi}\mathcal{E}_+ + \delta\mathcal{E}_- + \Gamma|\mathcal{E}_-|^2\mathcal{E}_- + 2\Gamma|\mathcal{E}_+|^2\mathcal{E}_- = 0 , \tag{19}$$

where for a thin-film stack the nonlinear parameter Γ is given by

$$\Gamma = \frac{4\pi\bar{n}\, n^{(2)}}{\lambda Z} , \tag{20}$$

where $n^{(2)}$ is the nonlinear refractive index (in m^2/W), and Z is the vacuum impedance (377 Ω). For waveguide and fiber geometries Γ is known as well [6, 12].

In the calculations to be presented the rejection band is centered around $\lambda = 930\,\text{nm}$. Furthermore, $n_{\text{GaAs}} = 3.59$, $n_{\text{AlAs}} = 2.97$ [14], so that from Eq. (3), $\bar{n} = 3.295$, and the layer thicknesses correspond to an optical path length of $\lambda/4$. Since the stack consists of 30 periods, $L = 4.3\,\mu\text{m}$ and the round-trip time equals 94 fs. Furthermore, from Eq. (6), $\kappa = 1.27\,\mu\text{m}^{-1}$ so that the grating's strength $\kappa L = 5.4$. Finally, $n^{(2)} = +3 \times 10^{-13}\,\text{cm}^2/\text{W}$ [15], giving $\Gamma = +3.5 \times 10^{-12}\,\text{mV}^{-2}$. Since the nonlinearity is positive, gap solitons are most easily generated near the high-frequency end of the rejection zone. The frequency of the incoming radiation is therefore chosen accordingly.

Figure 2 shows the intensity-dependent transmissivity for radiation with a detuning of $\delta = +107\,\text{THz}$, corresponding to a wavelength $\lambda = 885\,\text{nm}$, of the stack described above. Since branches with a negative slope are unstable against amplitude fluctuations, these have been indicated by dotted lines. Figure 2 shows the transmissivity for three different situations. The solid lines refer to a stack with a GaAs substrate and cover. The figure exhibits a low-intensity branch which exists for incoming intensities below about $36\,\text{GW/cm}^2$, and a high-intensity branch which is perfectly transmitting at about $13\,\text{GW/cm}^2$. It should be mentioned that previous work

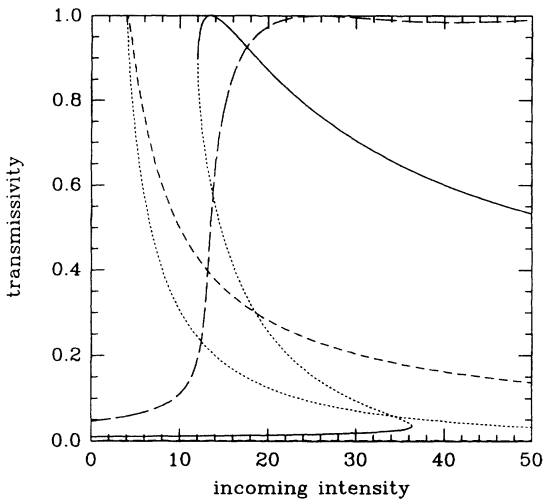

FIG. 2. Power-dependent transmissivity for the stack discussed in the text in three different situations. Dotted curves indicate branches which are unstable against amplitude fluctuations. Solid lines: with GaAs substrate and $\varphi = 0$. Since $n_1 = n_2 \approx \bar{n}$ in this case, the dependence on φ is weak. Short-dashed line: with air as substrate and cover, and $\varphi = 0$, leading to poor index matching. In fact, the lower branch extends to about $150\,\mathrm{GW/cm^2}$. Long-dashed line: with air as substrate and cover, and $\varphi = \pi$, leading to good index matching: The stack becomes transmissive at relatively low incoming intensities.

[2, 3] indicates that this upper branch may be unstable against the formation of sidebands. Since $n_1 = n_2 \approx \bar{n}$, the linear properties are only weakly dependent on φ [see the discussion following Eq. (10)], and the reflectivity vanishes at frequencies far from the rejection band [Eq. (16)]. The remaining curves give results for the stack with air (vacuum) both as substrate and as cover. Though this may be somewhat unrealistic, these curves were added because they clearly demonstrate the importance of the parameter φ. Equation (16) shows that since $n_1 = n_2 < \bar{n}$, the reflectivity vanishes for frequencies above the gap if $\varphi = \pi$, and below if $\varphi = 0$. Since the frequency is near the high-frequency side of the gap, these remaining curves show dramatic differences: If $\varphi = 0$ (short-dashed curve) the transmissivity is very poor, the low-transmission branch extends to about $140\,\mathrm{GW/cm^2}$, while if $\varphi = \pi$ (long-dashed curve), only about $15\,\mathrm{GW/cm^2}$ is required to reach the high-transmission regime.

Figures 3–7 show results of numerical simulations of pulse transmission. These are of particular interest since, at least with the presently available nonlinear materials, most of the gap-soliton experiments would have to make use of pulsed sources. In interpreting the results below using the cw results presented above it is important to keep in mind that for radiation inside the gap, the grating, in effect, has a high-quality Q, so transients die out very slowly on the time scale of a round-trip time. Since for the results presented below the pulse length is only a few round-trip times, the system does not get the time to settle in the steady states shown in Fig. 2. The required intensities for gap soliton formation are therefore found to be higher than the curves in the figure would imply.

All figures presented show the incoming (dotted lines), reflected (solid lines), and transmitted (dashed lines) energy flows as a function of time obtained from a numerical simulation of Eq. (19) [16]. Since the quantities given in the figures are energy flows and thus proportional to $n|\mathcal{E}_\pm|^2$, the area under the dotted curves (incoming radiation) equals the sum of that under the solid and dashed curves (reflected, transmitted radiation). The various figures differ by the choice of φ, by the choice of substrate and cover, as well as by the possible application of buffer layers to enhance the energy transfer. However, the shape and length of the energy pulse, and the intensity of the incoming pulse remain fixed: The incoming pulse is Gaussian and has a full width at half maximum (FWHM) of 200 fs, corresponding to 2.2 round-trip times and has a peak intensity of $40\,\mathrm{GW/cm^2}$. Also, the detuning of the center frequency of the pulse $\delta = +107\,\mathrm{THz}$ as above.

Figure 3 shows the quantities mentioned above as a function of time when the stack has a GaAs substrate and cover and $\varphi = 0$ and corresponds to the solid line in Fig. 2. No index matching occurs and the energy transfer between the stack and the surrounding media is thus poor, resulting in a low value for the transmitted energy.

Figures 4 and 5 show the results for the stack with air (vacuum) both as substrate and as cover (cf. Fig. 2) and $\varphi = 0, \pi$. Just as in Fig. 2 these show dramatic differences: If $\varphi = 0$ (Fig. 4) the transmittance is very poor, while for $\varphi = \pi$ (Fig. 5) a large fraction of the

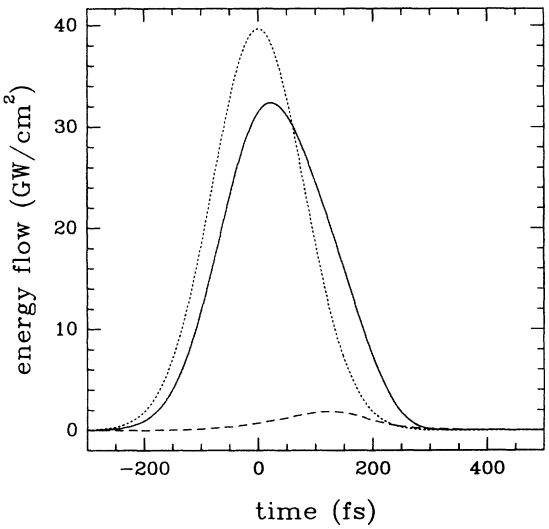

FIG. 3. Incoming (dotted line), transmitted (dashed line), and reflected (solid line) radiation as a function of time for a stack with parameters given in the text. The stack is embedded in GaAs and no buffer layers are applied. In addition, $\varphi = 0$. In this case only about 5% of the energy of the incoming radiation is transmitted. Since $n_1 = n_2 \approx \bar{n}$ in this case, the dependence on φ is small.

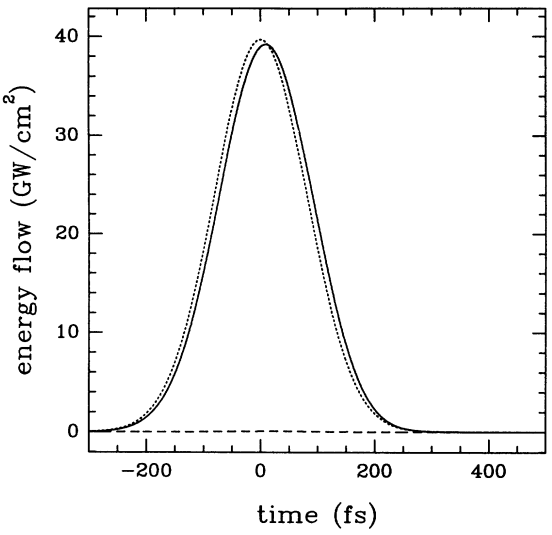

FIG. 4. Incoming (dotted line), transmitted (dashed line), and reflected (solid line) radiation as a function of time for a stack with parameters given in the text. Though perhaps not realistic, $n_1 = n_2 = 1$ here. Furthermore, $\varphi = 0$. Only about 0.2% of the incoming radiation is transmitted because the reflectivity vanishes at the low-frequency side of the gap.

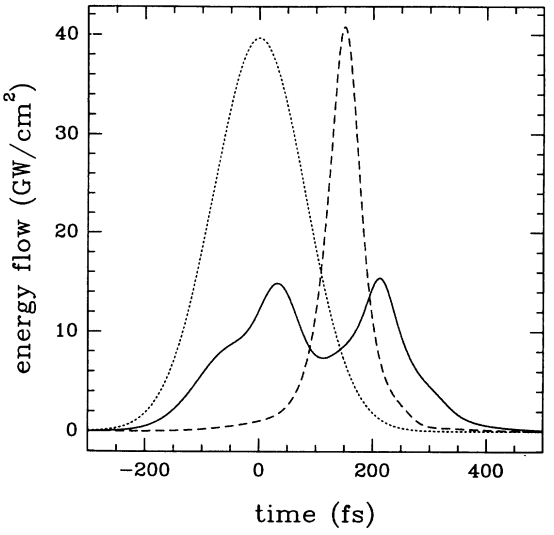

FIG. 6. Incoming (dotted line), transmitted (dashed line), and reflected (solid line) radiation as a function of time for a stack with parameters given in the text with a GaAs substrate and an air cover, and $\varphi = \pi$ ensuring index matching at the air interface. In this case about 43% of the incoming energy is transmitted.

incoming energy is transmitted and appears in a burst which is more intense than the incoming radiation. Also notice the time delay: The transmitted radiation peaks $1\frac{1}{2}$ round-trip times after the incoming radiation does so, indicating the slow energy transfer through the stack.

It should be mentioned that results similar to those in Figs. 4 and 5 are obtained in the (quite unrealistic) case in which $n_1 = n_2 = \bar{n}^2$, except that the transmittance is high if $\varphi = 0$ and low if $\varphi = \pi$. The index ratio of about 3 appears to be optimal: Equations (16) and (18) show

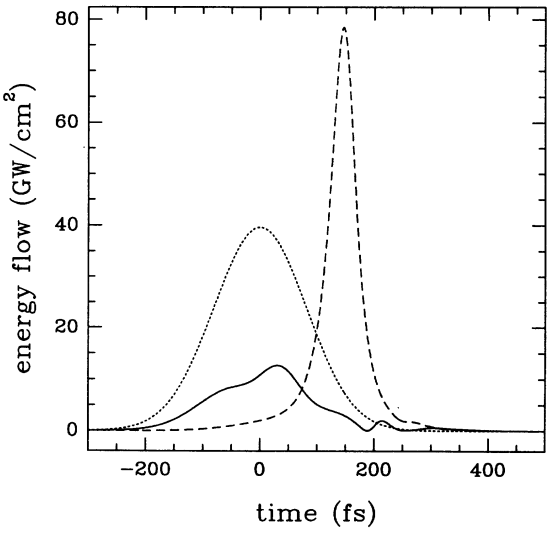

FIG. 5. Incoming (dotted line), transmitted (dashed line), and reflected (solid line) radiation as a function of time for a stack with parameters given in the text. Though perhaps not realistic, $n_1 = n_2 = 1$ here. Furthermore, $\varphi = \pi$. Now the reflectivity vanishes at the high-frequency side of the gap resulting in an efficient energy transfer between the gap soliton and the surrounding media (about 69% of the incoming energy is now transmitted).

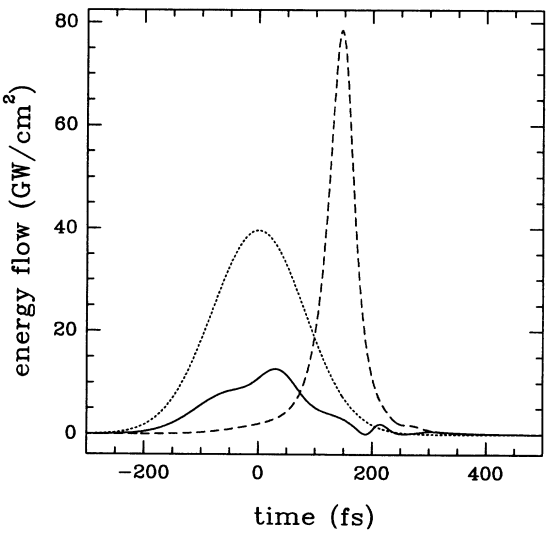

FIG. 7. Incoming (dotted line), transmitted (dashed line), and reflected (solid line) radiation as a function of time for a stack with parameters given in the text with a GaAs substrate and an air cover, and $\varphi = \pi$ ensuring index matching at the air interface. In addition, a buffer layer with a refractive index of 1.9 and optical path length of $\lambda/4$ was inserted between the stack and the substrate. About 69% of the incoming energy is now transmitted.

that if the index ratio is made larger the reflectivity vanishes at frequencies closer to the gap, but this minimum is too narrow to transmit enough of the radiation. But if the index ratio is smaller, the reflectivity vanishes at a frequency too far from the gap resulting in a small overlap with the frequency spectrum (though the minimum is quite wide now). Of course these conclusions depend in part on the pulse length and center frequency. Nevertheless, the optimum was found to be around 3 throughout.

I now consider the more realistic situation in which the substrate and the cover differ: $n_2 = 1$ (air cover), while $n_1 = 3.59$ (GaAs). As mentioned in Sec. II it is now impossible to match the indices at both the front and the back of the stack without a buffer layer. This is clearly seen in Fig. 6, in which no buffer layers are added and $\varphi = \pi$, ensuring index matching at the front of the system. It shows that though some of the incoming energy is transmitted, it is less than in Fig. 5. The reason is the index mismatch at the substrate interface. This can be directly confirmed from Fig. 6: The reflected energy exhibits two distinct peaks. These are due to the energy reflected of the front surface and that reflected at the substrate interface.

The energy transfer can be improved by adding a buffer layer between the substrate and the stack. Since good index matching occurs with air, the effective index of the stack is about unity, the index of the buffer should be $\sqrt{n_1} \approx 1.9$, and the optical path length $\lambda/4$ [7]. The result, with $\varphi = \pi$, is shown in Fig. 7 and clearly demonstrates an improvement in the energy transmission, and an overall response which is almost identical to that in Fig. 5.

IV. DISCUSSION AND CONCLUSIONS

It is clear from Sec. II that an analysis of the *linear* properties of the stack is crucial in order to optimize the energy transfer between gap solitons inside the structure and the surrounding media. This is perhaps somewhat surprising since solitons are profoundly *nonlinear*. However, as pointed out in Sec. III to lowest order the nonlinearity *shifts* the linear gap [11, 10], so that the linear properties remain important. To achieve efficient energy transfer it is of particular importance that the effective index of the linear stack be properly matched to those of the surrounding media. In Sec. III this was accomplished by an index ratio of about 3 and the proper choice for φ. It is, however, not clear at present how to make the *best* choice. Apart from the stack parameters, one can also vary the parameters of the incoming pulse. Most important of these is the pulse shape, length, power, center frequency, and, possibly, chirp.

While in all numerical examples in Sec. III the stack was taken to be symmetric ($\varphi = 0$, or π), this is of course by no means required. For other values of φ the stack is asymmetric, and according to Eq. (11) the effective index is then complex. As mentioned, proper matching with lossless materials is then impossible, so that energy transfer between gap solitons inside the stack and the surrounding media is never very efficient. Numerical simulations have shown that the results in general, and in particular the transfer efficiency, are between those for the two symmetric stacks. For this reason results for asymmetric stacks were not presented.

The results in Sec. III clearly show pulse reshaping and compression effects, particularly when a substantial fraction of the incoming energy is transmitted. This was earlier pointed out by Winful [6]. For incoming pulses which are more powerful than in the figures presented in Sec. II this compression becomes more pronounced, leading to a transmitted signal consisting of a single, very narrow and intense peak. For yet more powerful pulses both the reflected and the transmitted energy is concentrated in a number of different peaks. I expect to return to this situation in a future publication.

In conclusion, I have shown that gap solitons can be generated using external pulses which are incident on a nonlinear periodic medium. In order to minimize the required field strength it is important that the effective index of the stack be properly matched to the refractive indices of the surrounding media.

ACKNOWLEDGMENTS

The author is grateful to J.E. Sipe for many discussions during the initial stages of this work. He further thanks the members of the Centre for Theoretical Astrophysics at the University of Sydney for use of their computers.

[1] W. Chen and D.L. Mills, Phys. Rev. Lett. **58**, 160 (1987).
[2] C.M. de Sterke and J.E. Sipe, Phys. Rev. A **42**, 2858 (1990).
[3] H.G. Winful, R. Zamir, and S. Feldman, Appl. Phys. Lett. **58**, 1001 (1991).
[4] C.M. de Sterke and J.E. Sipe, Opt. Lett. **14**, 871 (1989).
[5] K.J. Blow, N.J. Doran, and B.K. Nayar, Opt. Lett. **14**, 754 (1989).
[6] H.G. Winful, Appl. Phys. Lett. **46**, 527 (1985).
[7] H.A. Macleod, *Thin-Film Optical Filters*, 2nd ed. (Hilger, Bristol, 1986), Chaps. 5 and 6.
[8] See, e.g., D. Marcuse, *Theory of Dielectric Optical Waveguides* (Academic, New York, 1974).
[9] M. Born and E. Wolf, *Principles of Optics*, 6th ed. (Pergamon, Oxford, 1980), p. 325.
[10] H.G. Winful, J.H. Marburger, and E. Garmire, Appl. Phys. Lett. **35**, 379 (1979).
[11] C.M. de Sterke and J.E. Sipe, Phys. Rev. A **38**, 5149 (1988).
[12] See, e.g., C.M. de Sterke and J.E. Sipe, J. Opt. Soc. Am. B **6**, 1722 (1989).
[13] J. He and M. Cada, IEEE J. Quantum Electron. **27**, 1182 (1991).
[14] H. Kressel and J.K. Butler, *Semiconductor Lasers and Heterojunction LED's* (Academic, New York, 1977), Chap. 10.
[15] M.C. Gabriel, H.A. Haus, and E.P. Ippen, J. Lightwave Technol. **LT-4**, 1482 (1989).
[16] C.M. de Sterke, K.R. Jackson, and B.D. Robert, J. Opt. Soc. Am. B **8**, 403 (1991).